 CMES, vol.13, no.2, pp.81-90, 2006

Treatment of Sharp Edges & Corners in the Acoustic Boundary Element Method under Neumann Boundary Condition

Zai You Yan[1]

Abstract: Boundary element method in acoustics for Neumann boundary condition problems including sharp edges & corners is investigated. In previous acoustic boundary element method, acoustic pressure and normal velocity are the two variables at sharp edges & corners. However, the normal velocity at sharp edges & corners is discontinuous due to the indefinite normal vector. To avoid the indefinite normal vector and the discontinuous normal velocity at sharp edges & corners, normal vector of elemental node is defined and applied in the numerical implementation. Then the normal velocity is transformed to velocity which is unique even at sharp edges & corners. Such treatments make sure that all variables in the acoustic boundary element method are definite. Computational efficiency and accuracy of the new model are demonstrated by three cases of interior acoustic problems for which analytical solutions can be found and one classical exterior acoustic radiation problem. Curvilinear quadrilateral isoparametric elements are applied in the computation. It is found that the numerical results agree with corresponding analytical solutions quite well.

keyword: Boundary element method, Sharp edge, Sharp corner, Normal velocity, Normal vector, Helmholtz integral equation

1 Introduction

Boundary element method is very suitable for the analysis of acoustic problems. Its significant advantages over other popular numerical techniques such as the finite difference and finite element method include a reduction of dimensionality of the problem by one, and an automatic satisfaction of the radiation boundary condition. However, the classical boundary element method has two main difficulties in the numerical implementation. One is for exterior acoustic problems it fails to provide a unique solution at certain frequencies, which are the characteristics of the associated interior problem. The nonuniqueness is a purely mathematical problem arising from the boundary integral formulation rather than from the nature of the physical problem. Detail description about the nonuniquness problem is presented by Ciskowski and Brebbia (1991). Another difficulty is at sharp edges & corners the normal vectors and normal velocities are indefinite or discontinuous. The discontinuity of normal vectors and normal velocities makes it very difficult to numerically implement the conventional boundary element method.

To date, a great deal of research has been conducted to overcome the nonuniqueness problem. The combined Helmholtz integral equation formulation (CHIEF) proposed by Schenck (1968) and the composite Helmholtz integral equation (CHIE) presented by Burton and Miller (1971) are the two most popular approaches. Seybert, Soenarko, Rizzo & Shippy (1985) provided a computational method based on the CHIEF method using isoparametric element formulation. Chen I.L., Chen J.T., Kuo S.R. & Liang M.T. (2001) extended the CHIEF method to the combined Helmholtz exterior integral equation formulation to solve the interior problems. Compared with the CHIEF method, the CHIE approach is more convenient and efficient in the numerical implementation. However it suffers from a major drawback that hypersingular integral is involved in the normal derivative of the Helmholtz integral equation. Review about numerical techniques for computing non-singular, nearly singular and nearly hyper-singular integrals was presented by Tanaka, Sladek V. & Sladek J. (1994). To date, many researchers have contributed on the hypersingular integral. Chien, Rajiyah & Atluri (1990) developed an approach to regularize the hypersingular integrals by employing certain known identities from the associated interior Laplace problems. This method was successfully implemented by Yang (1997) in the study of acoustic scattering across a wide frequency range. Liu and Rizzo (1992) developed a general form of the hypersingular boundary in-

[1] College of Aerospace Engineering, Nanjing University of Aeronautics and Astronautics, Yu Dao Street 29, City of Nan Jing, Jiang Su Province, P. R.China, 210016. Email: jutsjtu@yahoo.com.cn

tegral equation, which contained at most weakly singular integrals. Wu, Seybert & Wan (1991) implemented a regularized normal derivative equation, which converges in the Cauchy principal value sense rather than in the finite-part sense. Hwang (1997) regularized the hypersingular Helmholtz integral equation by some identities from the associated Laplace equations. Yan (2000), Yan, Jiang, He & Yan M. (2001), Yan, Hung & Zheng (2003) solved the hypersingular integral using the regularization relationship presented by Burton and Miller (1971). By introducing the concept of discretized operator matrix, evaluation of the double surface integrals was reduced to calculate the product of two discretized operator matrices. Such a treatment greatly improves the computational efficiency. Subsequently, taking the normal derivative of solid angles on the surface into account, a modified Burton and Miller's formulation was derived by Yan, Cui & Hung (2005). As a result, a more reasonable expression for the hypersingular operator was obtained. Theory and algorithm for the acoustic boundary element solver which can be used to get fast and stable solutions for boundary elements models on PCs under Windows was presented by Osetrov and Ochmann (2005). In their investigation, implementation of the Burthon and Miller regularization method for constant boundary elements was discussed. Recently, several novel boundary integral equations are derived and implemented to avoid the hypersingular integral. Qian, Han & Atluri (2004) and Qian, Han, Ufimtsev & Atluri (2004) derived the symmetric Galerkin boundary element formulations of the regularized forms of non-hypersingular boundary integral equations. Meantime, they presented the non-hypersingular boundary integral equations by the collocation based boundary element method. Acoustic scattering from complex shaped three dimensional structures was investigated by Chandrasekhar and Rao using the MoM approach. Then Chandrasekhar (2005) calculated the acoustic fields scattered by three dimensional rigid bodies of arbitrary shape.

Investigation on the indefinite normal vectors and discontinuous normal velocities at sharp edges & corners is very few. Usually node on sharp edge or corner is replaced by two or more separate nodes close to it. Then one has to modify the mesh and wonder how large the gap between these separate nodes should be to make sure the convergence of solutions. Wu, Seybert & Wan (1991) placed the collocation points inside each element to avoid the indefinite normal vectors. The final overdetermined linear equation system was solved by a least-square procedure. The work presented by Gray and Lutz (1990) is very notable. In their studies, a corner is discretized using multiple nodes. The necessary additional equations for extra nodes were formed by using the interior and exterior limit of differentiating the Helmholtz integral equation. Besides, Wang, Atalla & Nicolas (1997) discretized a corner as double nodes and evaluate the equation directly by taking its left-hand and right-hand limits at the corner. To avoid overdetermined linear equations, they assumed two independent pressure variables at each of the corners.

In this paper, acoustic boundary element method for problems with sharp edges & corners is investigated. As stated above, at sharp edges & corners the normal vector is indefinite and the normal velocities are discontinuous. New technique is developed by applying the definition of normal vector of elemental node and then transforming normal velocity to velocity. As a result, all the variables are definite on the structure surfaces and the nodes on sharp edges & at corners need not to be divided into several nodes. No need to take limitation any more. This paper is organized into five sections. Following the introduction, theoretical formulation of the governing equation for acoustic propagation in interior domain is presented. Next, treatment of the indefinite normal vectors and discontinuous normal velocities at sharp edges & corners is presented. Normal vector of elemental node is defined and applied. Then the discontinuous normal velocity is transformed to the velocity. In the subsequent section, numerical calculations are performed for interior problems of straight duct vibration and a complex structure with re-entrant corners and exterior problem of radiation of a finite cylinder. Finally a conclusion is drawn.

2 Conventional helmholtz integral equation

Consider the interior acoustic problem under Neumann boundary conditions. The interior fluid medium is assumed to be homogeneous with density ρ. Sound travels in the fluid medium with speed c. The normal vector $\vec{n}$ at any point on the surface is taken to be the outward normal as shown in Fig. 1. For convinience, element numbers are shown in this figure.

The governing differential equation [Ciskowski and Brebbia (1991)] in the interior domain in steady-state lin-

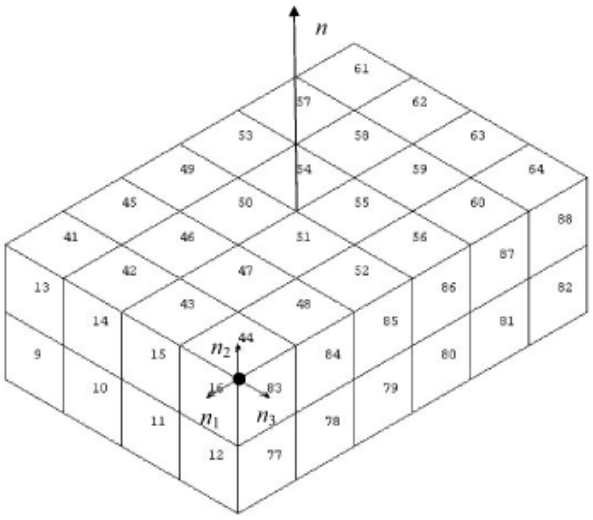

Figure 1 : Normal vector and normal vector of elemental node for structure with sharp edges & corners.

ear acoustics is the well-known Helmholtz equation,

$$\left(\nabla^2 + k^2\right)\varphi = 0 \tag{1}$$

Neumann boundary condition on the boundary surface S can be expressed as,

$$\frac{\partial \varphi}{\partial n} = -i\omega\rho v_n \tag{2}$$

where φ represents the acoustic pressure, ω represents the circular frequency, k is the wavenumber and $v_n$denotes the normal surface velocity.

By using the Green's second identity, the surface Helmholtz integral equation is expressed as

$$\iint \left(\varphi(q)\frac{\partial G_k(p,q)}{\partial n_q} - G_k(p,q)\frac{\partial \varphi(p)}{\partial n_q}\right) dS_q = c(p)\,\varphi(p) \tag{3}$$

The free-space Green's function G_k for the three-dimensional wave equation is

$$G_k(p,q) = e^{-ikr}/4\pi r, \qquad r = |p-q| \tag{4}$$

Where p is the source point on the surface and q is the field point on the surface. r represents the Euclidean distance between points p and q.

Solid angle $c(p)$ is given by

$$c(p) = -\iint \frac{\partial G_0(p,q)}{\partial n_q} dS_q \tag{5}$$

where

$$G_0(p,q) = 1/4\pi r \tag{6}$$

In operator notation [Mathews (1986)], the above equation can be written as

$$\left[c(p)\,I + M_k\right]\varphi = L_k\frac{\partial \varphi}{\partial n} \tag{7}$$

where I is the identity integral operator, and

$$L_k\mu = \iint \mu(q) G_k(p,q) dS_q \tag{8}$$

$$M_k\mu = \iint \mu(q)\frac{\partial G_k(p,q)}{\partial n_q} dS_q \tag{9}$$

For acoustic exterior problems, the surface Helmholtz integral equations can be found in the references presented by Ciskowski and Brebbia (1991), Yan (2000) and Yan, Hung & Zheng (2003).

3 Treatment of the indefinite normal vector and discontinuous normal velocity at sharp edges & corners

Here only Neumann boundary conditions are considered. At sharp edges or corners, direction of the given velocity is denoted by $\vec{v}$. Then the velocity can be expressed as $V\vec{v}$. At the corner node shown in Fig. 1 by a black dot, there are three elements, 16, 44 and 83 who contain this node. On each element, normal vector of this corner node is represented by $\vec{n}_1$, $\vec{n}_2$, $\vec{n}_3$ respectively. Here $\vec{n}_1$ is defined as normal vector of elemental node for this corner node on element 16. Therefore $\vec{n}_2$ is the normal vector of elemental node for this corner node on element 44 and $\vec{n}_3$ is the normal vector of elemental node for this corner node on element 83. This definition can be applied to any node at sharp edges & corners. For node on edges shown in Fig 1, there are two different normal vectors of elemental node. Using the definition of normal vector of elemental node, normal velocity at each elemental node can be expressed as

$$V_{ni} = V\vec{v}\cdot\vec{n}_i = \left(\vec{v}\cdot\vec{n}_i\right)V = V\cos\alpha_i \quad i = 1,2,3 \tag{10}$$

where α_i is the angle between the direction of the velocity and the normal vector of elemental node.

Applying Eq. (11), the surface Helmholtz integral equation (4) can be re-written in operator notation as,

$$[c(p)I + M_k]\varphi = L_{kv_n}V \tag{11}$$

where

$$L_{kv_n}\mu = -i\omega\rho \iint \mu(q)G_k(p,q)\cos\alpha_i dS_q \tag{12}$$

$\vec{n}_i$ represents normal vector of elemental node.

In Eq. (12), there are two variables φ and V both of which are definite at sharp edges & corners. Therefore the problem of indefinite normal vector and discontinuous normal velocity at sharp edge & corners is overcome. To differentiate the new model from the conventional surface Helmholtz integral equation, the conventional Helmholtz integral equation is termed as (φ, v_n) model, while the new model is termed as (φ, V) or $(\varphi, |\nabla\varphi|)$ model. Finally the linear equation system is numerically solved using a weakly singular integration scheme, such as that proposed by Lachat and Watson (1976).

Although the above Eqs. (11), (12) and (13) are very simple, they are of great importance. Eq. (11) points out that at sharp edge & corner, even if at the same global node the normal velocities may be different on different elements. Therefore in the conventional acoustic boundary element method in which normal velocity is taken as the variable, assembly of the coefficient matrices can not be done. While, in the Eqs. (12) and (13) because the variable is transformed to the amplitude of velocity, it is easy to assemble the coefficient matrices. Moreover, Eqs. (11) to (13) precisely describes the piecewise smooth property of the structure. That is although normal vectors are not discontinuous at some nodes; they are continuous over each element.

Gray and Lutz (1990) stated that for more complicated surface structure, as in the corner point of a cube, additional nodes would be employed, the number depending upon how many separate normal directions exist at the corner. But from Eq. (12), we find that no matter how many separate normal directions exist at the corner, additional equations to be employed are not more than three.

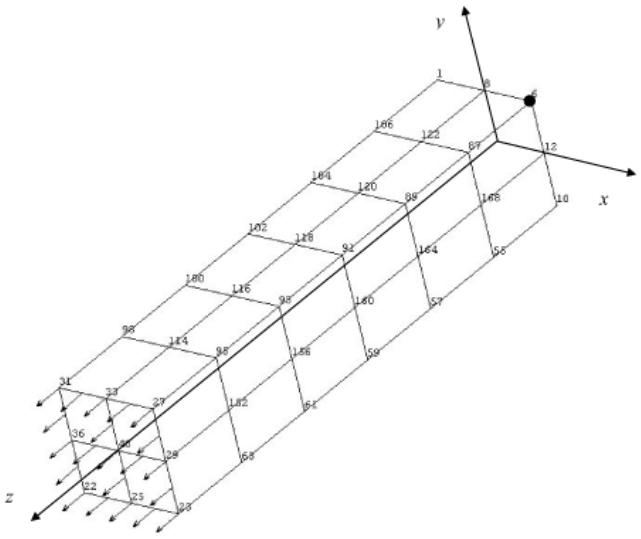

Figure 2 : Mesh for straight duct vibrating with unit normal velocity on the inlet surface.

4 Numerical examples

In order to test the accuracy and efficiency of the new technique, three cases of interior acoustic problems and one of exterior acoustic problem have been computed. The fluid medium in all the four cases is air. The first example is a straight channel [Wu (2000)] vibrating with a unit normal velocity on the inlet surface and an anechoic termination at the outlet as shown in Fig. 2. For the convenience of understanding, the unit normal velocity on the inlet surface and part of node numbers are also displayed in this figure. Size of the straight duct is $(5\times5\times25)$ cm. Coordinate origin is located at the center of the outlet surface. There are 56 elements and 170 nodes in total. In the second example, the structure is the same as the first one, but distribution of the surface velocities is generated by a virtual pulsating sphere [Provatidis and Zafiropoulos (2002)] located at point $(0,0,-0.1)\,m$ in the exterior domain. The third example is computed to take the re-entrant corners [Gray and Lutz (1990)] into account. Model for this example is shown in Fig. 3. There are 168 elements and 506 nodes in total. Same as in the second case, distribution of the surface velocities is generated by a virtual pulsating sphere located at point $(0,0,-0.1)$ in the exterior domain. For convenience, some of node numbers are displayed. Size of the structure is $l_{59,232} = 5$ cm, $l_{132,248} = 2$ cm, $l_{196,160} = 2$ cm, $l_{232,248} = 2$ cm and $l_{59,160} = 1$ cm, where the subscripts

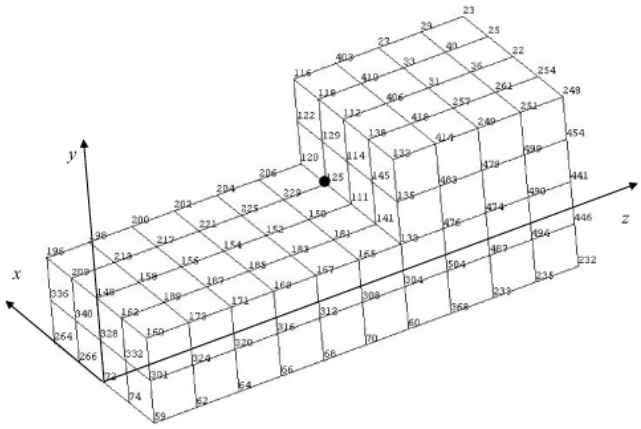

Figure 3 : Mesh for structure with re-entrant corners.

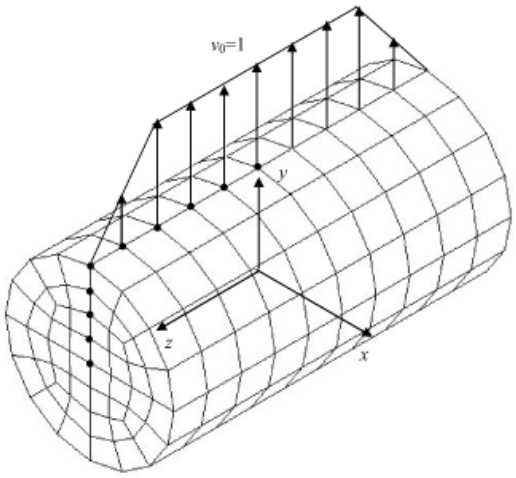

Figure 4 : Mesh for a finite cylinder.

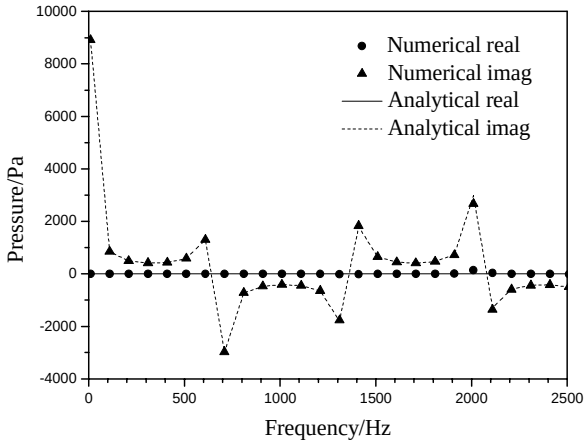

Figure 5 : Frequency response at the corner node 6 for the straight duct vibrating on the inlet surface.

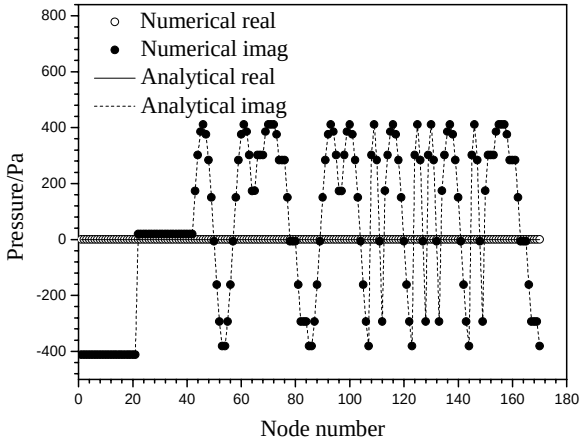

Figure 6 : Surface acoustic pressures at each node as frequency equals to 1010 Hz for the straight duct vibrating on the inlet surface.

are corresponding node numbers. Finally a classical example presented by Copley (1967), Fenlon (1969) and Wang, Atalla & Nicolas (1997) is simulated, as shown in Fig. 4. There are 256 elements and 770 nodes in total. It is the radiation problem of a finite cylinder of radius a and length $2L$ with a=0.5$L$and$L$=1. The end caps of the cylinder are considered to be clamped and the velocity profile [Fenlon (1969)] over the cylindrical surface is taken as unity in the range $[-0.8L \le z \le 0.8L]$. Beyond this range, the velocity profile tapers off linearly to zero at the end edges as shown in Fig. 4. In all the examples, the surfaces are modeled using curvilinear quadrilateral isoparametric elements as shown in Fig. 2 to Fig. 4. Models are generated by commercial available software, such as Hypermesh, Ansys. Then the examples are computed using the in-house developed code, SSFI (Sound Structure Fluid and their Interaction). This software is suitable to solve multi-domain acoustic problems, especially the problems of structural-acoustic interaction.

4.1 Straight duct vibrating with unit normal velocity on the inlet surface

The analytical solution of acoustic pressure $\varphi(z)$ for interior problem of a straight duct vibrating with a unit normal velocity v_0 on the inlet surface shown in Fig. 2 is given by

$$\varphi = \frac{i\rho c v_0}{\sin kl}\cos kz \tag{13}$$

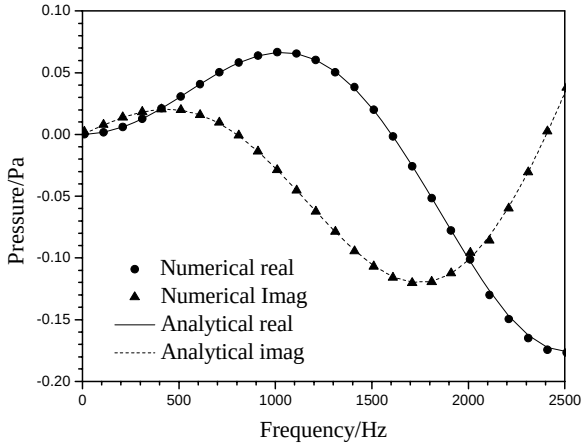

Figure 7 : Frequency response at the corner node 6 for the straight duct vibrating with velocities generated by a pulsating sphere at z=0.1.

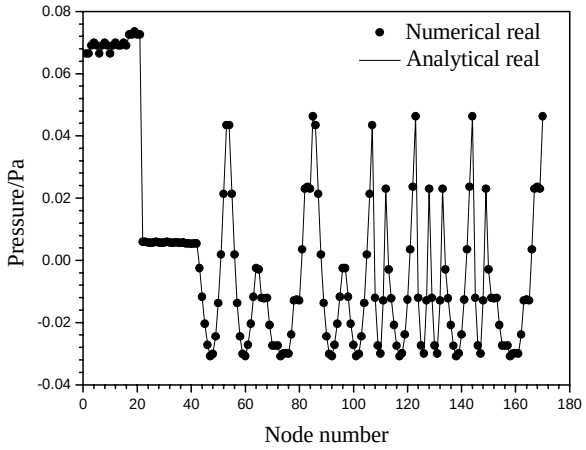

Figure 8 : Real part of surface pressures at each node as frequency equals to 1010 Hz for the straight duct vibrating with velocities generated by a pulsating sphere at z=0.1.

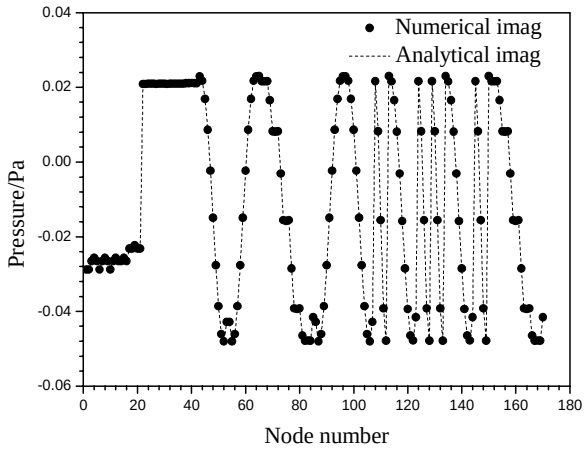

Figure 9 : Imaginary part of surface pressures at each node as frequency equals to 1010 Hz for the straight duct vibrating with velocities generated by a pulsating sphere at z=0.1.

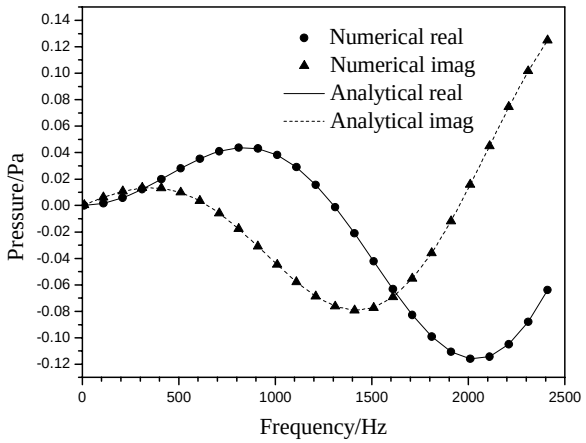

Figure 10 : Frequency response at the corner node 125 for structure with re-entrant corners.

where ρ and c are the fluid density and sound velocity respectively. k is wave number. l is the length of the straight duct along $z$direction.

Frequency response of acoustic pressures at the corner node 6 marked by a black dot in Fig. 2 is displayed in Fig. 5. The frequency range is from 10 to 2410 Hz with frequency step 100 Hz. Analytical solutions are obtained in the same frequency range and with the same frequency step. Comparison between numerical results and the analytical solutions shows that the new model works well. In Fig. 6, acoustic pressures at each node as frequency equals to 1010 Hz are presented. Such figures are very useful to programmer, because they can be used to check the symmetry and trend of solutions. Clearly, the numerical results agree greatly well with corresponding analytical solutions. This figure demonstrates that the new model works well at every node.

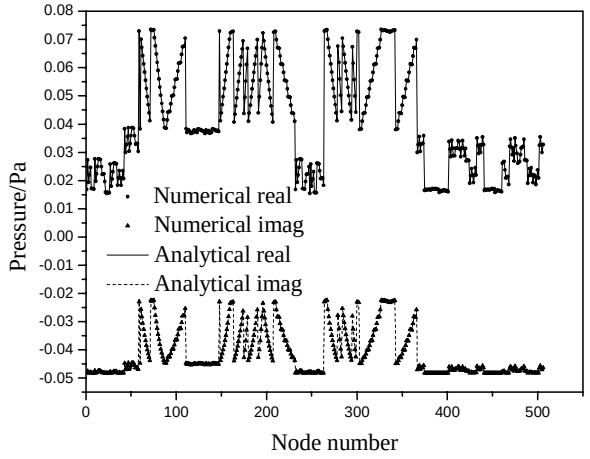

Figure 11 : Surface acoustic pressures at each node as frequency equals to 1010 Hz for structure with re-entrant corners.

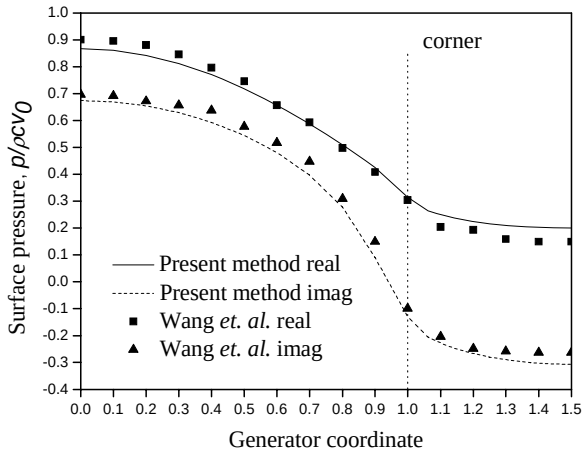

Figure 12 : Surface acoustic pressures for radiation of a finite cylinder at wave number kL=2.

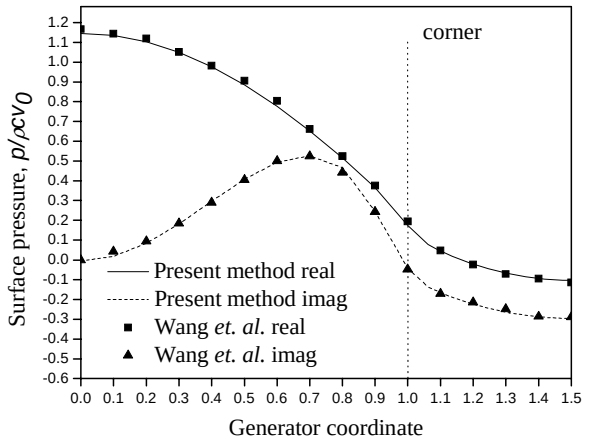

Figure 13 : Surface acoustic pressures for radiation of a finite cylinder at wave number kL=4.

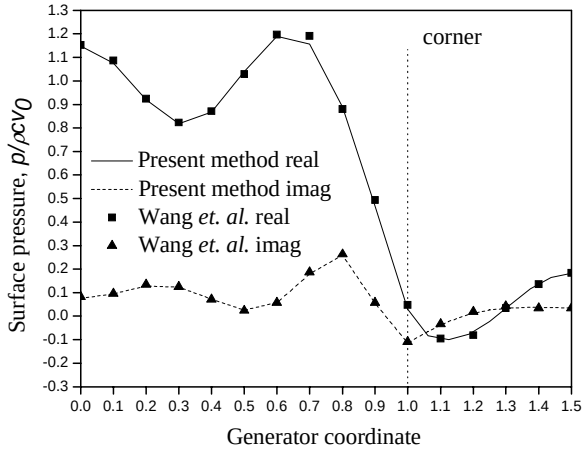

Figure 14 : Surface acoustic pressures for radiation of a finite cylinder at wave number kL=10.

4.2 Straight duct vibrating with velocities generated by a virtual pulsating sphere

In this case, the structure is the same as the above one as shown in Fig. 2. Distribution of surface velocities are generated by a virtual pulsating sphere located in the exterior domain at the point (0, 0, -0.1). Velocities generated by a pulsating sphere are given by

$$\vec{V} = \frac{(1+ikr)}{r^3} e^{-ik(r-a)} \frac{a^2 U_a}{1+ika} \vec{r} \tag{14}$$

Pressures generated by the pulsating sphere are given by

$$\varphi(r) = \frac{a}{r} U_a \frac{i\rho cka}{1+ika} e^{-ik(r-a)} \tag{15}$$

Because Eq. (16) satisfies both the governing Eq. (1) and the boundary condition Eq. (2), it is the analytical solution for structure vibrating with the surface velocity distribution given by Eq. (15).

Radius of the virtual pulsating sphere is $a = 1mm$ and its surface velocity $U_a = 1 \quad m/s$. Frequency response of surface acoustic pressures at the corner node 6 marked

by a black dot in Fig. 2 is displayed in Fig. 7. The frequency range is from 10 to 2410 *Hz* with step 100 *Hz*. Comparison between the numerical results and corresponding analytical solutions shows that the new model works very well. In Figs. 8 and 9, real and imaginary parts of surface acoustic pressures at each node are presented and compared with the corresponding analytical solutions. Clearly the numerical results agree with the analytical solutions greatly well. These figures demonstrate that the new model does work at sharp edges & corners.

4.3 Structure with re-entrant corners vibrating with velocities generated by a virtual pulsating sphere

To take into account of re-entrant corners, interior acoustic problem for structure including re-entrant corners [Gray and Lutz (1990)] is simulated. Similarly, surface velocity distribution is generated by a virtual pulsating sphere located at the point (0, 0, -0.1) in the exterior domain. Therefore the surface velocities and analytical surface acoustic pressures can be obtained by Eqs. (15) and (16).

Frequency response of surface acoustic pressures at the node 125 on the re-entrant edge marked by a black dot in Fig. 3 is displayed in Fig. 10. The frequency range is from 10 to 2410 *Hz* with step 100 *Hz*. Comparison between numerical results and analytical solutions is also presented in this figure. In Fig. 11, surface acoustic pressures at each node as frequency equals to 1010 Hz are presented. Once more, the comparison between numerical results and analytical solutions shows that the new model works very well.

4.4 Radiation of a finite cylinder

In the above, three interior acoustic problems have been computed. Here the exterior acoustic radiation of a finite cylinder is simulated. This case once computed by Copley (1967), Fenlon (1969) and Wang, Atalla & Nicolas (1997). Unlike Copley (1967) and Fenlon (1969), Wang, Atalla & Nicolas (1997) applied the fundamental solution $e^{-ikr}/4\pi r$ instead of $e^{ikr}/4\pi r$. As a result, their numerical results for acoustic pressure should be the conjugate of those obtained by Copley (1967) and Fenlon (1969). In this paper, the fundamental solution $e^{-ikr}/4\pi r$ is applied, so the numerical results will be the conjugate of those obtained by Copley (1967) and Fenlon (1969). For simplicity, the numerical results are only compared to those obtained by Wang, Atalla & Nicolas (1997) at wave numbers kL=2, 4 and 10. The generator coordinated applied by Wang, Atalla & Nicolas (1997) is used. Because of symmetry, only half of the generator line is displayed as shown in Fig. 4 by the black dots. Figs. 12 to 14 display the comparison between the numerical results obtained using the present model and those obtained by Wang, Atalla & Nicolas (1997). Obviously, these two kinds of numerical results agree very well. This example validates the efficiency and correctness of new model once more.

5 Conclusion

Normal vector of elemental node is defined and applied. Then the variable v_n in the conventional Helmholtz integral equation is transformed to the variable V which is definite on all the structure surfaces. As a result, the indefinite normal vector and discontinuous normal velocities at sharp edges & corners are overcome. To differentiate the new model from the conventional Helmholtz integral equation, the conventional Helmholtz integral equation is termed as (φ, v_n)model and the new model is termed as (φ, V) or $(\varphi, |\nabla\varphi|)$ model. The idea presented in this paper is very easy to be implemented in program and no additional nodes to be employed. Four examples are computed to test the correctness of the new technique. Comparison between numerical results and corresponding analytical solutions and results obtained by other researchers show that the new technique works quite well. The new technique can be applied to boundary element method in other research fields. As stated in the title, only problems under Neumann boundary conditions are investigated. For problems under Dirichlet boundary conditions or hybrid boundary conditions, it will be very complicated to apply this new technique.

Acknowledgement: This project was supported by Nanjing University of Aeronautics and Astronautics Talent Development Foundation.

References

Burton A.J.; Miller G.F. (1971): The application of integral equation methods to the numerical solution of some exterior boundary value problems. *Proc.R.Soc.London Ser.* A323: 201-210.

Chandrasekhar B. (2005): Acoustic scattering from

arbitrarily shaped three dimensional rigid bodies using method of moments solution with node based basis functions. *CMES: Computer Modeling in Engineering & Sciences* 9(3): 243-253.

Chandrasekhar B.; Rao S.M. (2005): Acoustic scattering from complex shaped three dimensional structures. *CMES: Computer Modeling in Engineering & Sciences* 8(2): 105-117.

Chen I.L.; Chen J.T.; Kuo S.R.; Liang M.T. (2001): A new method for true and spurious eigensolutions of arbitrary cavities using the combined Helmholtz exterior integral equation formulation method. *J. Acoust. Soc. Am.* 109: 982-998.

Chien C.C.; Rajiyah H.; Atluri S.N. (1990): An effective method for solving the hypersingular integral equations in 3-d acoustics. *J. Acoust. Soc. Am.* 88: 918-937.

Ciskowski R.D.; Brebbia C.A. (1991): *Boundary element methods in acoustics.* Computational Mechanics Publications, Souththampton Boston: 65-75.

Copley L.G. (1967): Integral equation method for radiation from vibrating bodies. *J. Acoust. Soc. Am.* 41: 807-816

Fenlon H.F. (1969): Calculation of the acoustic radiation field at the surface of a finite cylinder by the method of weighted residuals. *Proc. IEEE* 57: 291-306.

Gray L.J.; Lutz E. (1990): On the treatment of corners in the boundary element method. *J. Comput. Appl. Math.* 32: 369-386.

Hwang W.S. (1997): Hypersingular boundary integral equations for exterior acoustic problems. *J. Acoust. Soc. Am.* 101: 3336-3342.

Lachat J.C.; Watson J.O. (1976): Effective numerical treatment of boundary integral equations. *Int. J. Num. Methods Eng.* 10: 991-1005.

Liu Y.J.; Rizzo F.J. (1992): A weakly-singular form of the hypersingular boundary integral equation applied to 3-D acoustic wave problems. *Comput. Methods Appl. Mech. Eng.* 96: 271-287.

Mathews I.C. (1986): Numerical techniques for three dimensional steady-state fluid-structure interaction. *J. Acoust. Soc. Am.* 79: 1317-1325.

Osetrov A.V.; Ochmann M. (2005): A fast and stable numerical solution for acoustic boundary element method equations combined with the Burton and Miller method for models consisting of constant elements. *J. Comput. Acoust.* 13(1): 1-20.

Provatidis Ch.; Zafiropoulos N. (2002): On the 'interior Helmholtz integral equation formulation' in sound radiation problems. *Eng. Anal. Bound. Elem.* 26: 29-40.

Qian Z.Y.; Han Z.D.; Atluri S.N. (2004): Directly derived non-hypersingular boundary integral equations for acoustic problems, and their solution through Petrov-Galerkin schemes. *CMES: Computer Modeling in Engineering & Sciences* 5(6): 541-562.

Qian, Z.Y.; Han, Z.D.; Atluri, S.N. (2004): Erratum: "Directly derived non-hypersingular boundary integral equations for acoustic problems, and their solution through Petrov-Galerkin schemes" (*CMES: Computer Modeling in Engineering & Sciences,* vol 5, no. 6, pp 541-562, 2004). *CMES: Computer Modeling in Engineering & Sciences* 6 (1): 115-122.

Qian Z.Y.; Han Z.D.; Ufimtsev P.; Atluri S.N. (2004): Non-hypersingular boundary integral equations for acoustic problems, implemented by the collocation-based boundary element method. *CMES: Computer Modeling in Engineering & Sciences* 6(2): 133-144.

Schenck H.A. (1968): Improved integral formulation for acoustic radiation problems. *J. Acoust. Soc. Am.* 44: 41-58.

Seybert A.F.; Soenarko B.; Rizzo F.J.; Shippy D.J. (1985): An advanced computational method for radiation and scattering of acoustic waves in three dimensions. *J. Acoust. Soc. Am.* **77**: 362-368.

Tanaka M.; Sladek V.; Sladek J. (1994): Regularization techniques applied to boundary element methods. *ASME Appl. Mech. Rev.* 47(10): 457-499.

Wang W.P.; Atalla N.; Nicolas J. (1997): A boundary integral approach for acoustic radiation of axisymmetric bodies with arbitrary boundary conditions valid for all wave numbers. *J. Acoust. Soc. Am.* 101: 1468-1478.

Wu T.W. (2000): *Boundary Element Acoustics: Fundamentals and Computer Codes.* WIT, Southampton: 111-112.

Wu T.W.; Seybert A.F.; Wan G.C. (1991): On the numerical implementation of a Cauchy principal value integral to insure a unique solution for acoustic radiation and scattering. *J. Acoust. Soc. Am.* 90: 554-560.

Yan Z.Y. (2000): *Sound transmission through thin elastic shell with different fluids on both the inside and outside*. Ph. D Thesis, Shanghai Jiao Tong University, P.R.

China.

Yan Z.Y.; Cui F.S.; Hung K.C. (2005): Investigation on the Normal Derivative Equation of Helmholtz Integral Equation in Acoustics. *CMES: Computer Modeling in Engineering & Sciences,* 7(1):97-106.

Yan Z.Y.; Hung K.C.; Zheng H. (2003): Solving the hypersingular boundary integral equation in three-dimensional acoustics using a regularization relationship. *J. Acoust. Soc. Am.* 113: 2674-2683.

Yan Z.Y.; Jiang J.; He Y.S.; Yan M. (2001): New approach used to deal with hypersingular numerical integral in acoustic boundary element method. *Shengxue Xuebao/Acta Acustica* (in Chinese) 26: 282-286.

Yang S.A. (1997): Acoustic scattering by a hard and soft body across a wide frequency range by the Helmholtz integral equation method. *J. Acoust. Soc. Am.* 102: 2511-2520.